Polymer Bulletin
https://doi.org/10.1007/s00289-022-04619-y

ORIGINAL PAPER

Synthesis of polyurethane acrylate hybrids containing fluorine and siloxane by the sol–gel method for UV-curable coatings

Mert Çınar[1] · **Sevim Karataş**[1]

Received: 7 July 2022 / Revised: 17 November 2022 / Accepted: 22 November 2022

Abstract

In this study, five different UV-curable polyurethane acrylate (PUA) resins (B, H:20, H:40, P:10/H:20, and P:20/H:40) were synthesized using different amounts of polyols [(2,2-bis(4-β-hydroxyethoxy) phenyl 6F propane (HEPFA); polydimethylsiloxane (PDMS); propylene glycol) which reacted with isophorone diisocyanate (IPDI) and end-capped with 2-hydroxyethyl methacrylate (HEMA). Then, a series of UV-curable PUA formulations and their nano-hybrids (B/S10-30, H20/S10-S30, H40/S10-S30, P10:H20/S10-S30, P20:H40/S10-S30) were prepared by the sol–gel method using different amounts of sol–gel solutions. The obtained formulations were cured with UV rays. The effects of PDMS, HEPFA and sol–gel content on the physical, thermal and mechanical properties of the UV-curable PUA coatings were investigated. When the HEPFA, PDMS and sol–gel content were increased in the urethane base formulation (B), the gloss increased from 98° to 117°, 133° and 137° for B, H40, P20:H40 and P20:H40/S30, respectively. TGA analysis showed that the decomposition temperatures shifted significantly upward with increasing amounts of HEPFA, PDMS and the sol–gel precursor. The water absorption of the hybrids decreased from 4.7 wt% (B) to 2.5 wt% (P20:H40/S30). The nano-hybrid coatings exhibited higher contact angle values for deionized water/ethylene glycol compared to the pure PUAs, ranging from 52°/48° (B) to 78°/76° (P20:H40/S30). The SEM analysis showed that the nano-silica particles were scattered in the polymer matrix without serious agglomeration when 30 wt% of sol–gel solution was added to B, H40 and P20:H40. These results indicate that the overall properties of the PUAs and their hybrids were improved and that they could potentially be used as coatings in practical applications.

Keywords Polyurethane acrylate · Coating · UV-curing · Sol–gel technique · Hybrid materials

✉ Sevim Karataş
skaratas@marmara.edu.tr

Extended author information available on the last page of the article

Published online: 13 December 2022

Introduction

As one of the most popular resins, polyurethane acrylate (PUA) is a significant class of UV-curable oligomers and can exhibit a wide range of properties due to its versatility in shaping its molecular structure [1–3]. PUA is based on a polyurethane oligomer end-capped with an acrylic functionality and is widely used in protective coatings because it can form a coherent film on material surfaces, giving them an aesthetic appearance and protecting them from environmental effects, as well as increasing their strength and durability. To date, there are many ways to improve the hardness and physical properties of coatings by modifying PUA. These include increasing the crosslink density, improving hydrogen bonding, adding rigid groups and nanoparticles to the matrix, and converting linear PUA to hyperbranched PUA [4–9].

UV curing technology has gained attention mainly due to stricter global regulations on volatile organic compounds (VOC). It is not only an environmentally friendly technique, but also offers many advantages such as versatility, instant drying, and fast and efficient polymerization [10–12]. This makes UV curing ideal for a variety of practical applications, including coatings, overlay varnishes, inks, 3D printing, and adhesives. In the market, UV-curable oligomers hold the largest share by composition due to their low cost and ease of use, as well as their high mechanical and bulk properties, and resistance to chemicals. The final properties of the coatings are highly dependent on these functionalized oligomers, which can be acrylated epoxies, ethers, esters, and urethanes [13–17].

Numerous studies have shown that the sol–gel approach, a commonly used method to prepare organic–inorganic (O–I) nano-hybrid materials, effectively increases the hardness of coatings [18–21]. Nevertheless, homogeneous dispersion of the inorganic nanoparticles in the organic matrix is crucial for UV-curable PUA nanocomposite coatings. The sol–gel method can be used to incorporate silica nanoparticles into polymers by forming a three-dimensional Si–O-Si network through hydrolysis and polycondensation of silica alkoxides. This leads to a strong interaction between the silica nanoparticles and polymer matrix, as well as an increase in crosslink density, which significantly improves the physical properties of the polymers, such as mechanical strength, abrasion resistance, and solvent resistance [21–25].

PU coatings can also be improved by attaching siloxane units (–Si–O–) to the PU backbone. Poly(dimethylsiloxane) (PDMS) has some superior properties such as low surface free energy, good adhesion and water resistance, high thermal and UV stability, non-toxicity and low cost [26–30]. It has been reported that PU, which consists only of PDMS chains in the polymer backbone, is brittle and cannot be used as a coating material. To achieve high properties, a combination of PDMS and another macrodiol (e.g., polyether, polyester) is usually used as a mixture in the PU coatings. As a result, the prepolymer of PU achieves higher molecular weights and better mechanical properties [28, 30, 31].

Another way to improve the thermal stability and hydrophobicity of PU coatings is to incorporate fluorinated blocks into the PU structure. The small size and high

electronegativity of the fluorine atom lead to a strong C-F bond (485 kJ/mol) in contrast to C–H (411 kJ/mol), C–C (346 kJ/mol), and C–N bonds (305 kJ/mol) [32–36]. The strongly polarized C–F bonds of fluorine, combined with its low intermolecular attraction, make fluorine-containing materials attractive for their low surface energy, low refractive index, high thermal stability, and weather resistance [37–41]. However, their content in the PU structure could be minimized due to their high cost.

There are numerous studies on UV-curable polyurethane hybrid materials containing fluorine and siloxane molecules [42–47]. However, UV-curable PUAs containing HEPFA and PDMS, combined with silica nanoparticles, have not yet been published in the literature. This study aimed to prepare a series of UV-cured nano-hybrid PUA coating materials containing fluorine and silicone via the sol–gel method. For this, five different UV-curable PUA oligomers were synthesized and UV-cured nano-hybrid coatings were prepared by adding the sol–gel solution at different rates to the obtained oligomers. In this study, silicone and fluorine atoms were introduced into the polymer backbone using HEPFA and PDMS monomers, respectively. Nano-silica particles were also inserted into the polymer network using the sol–gel method. The structures of the PUA oligomers were characterized by FT-IR and ^{1}H-NMR analyzes. In addition, the synergistic effects of HEPFA, PDMS, and the sol–gel solution on the physical, thermal, mechanical, and morphological properties of the polyurethane hybrid coating materials were investigated.

Experimental

Materials

Bisphenol-AF (BP-AF; 4,4′-(hexafluoroisopropylidene)-diphenol) and isophorone diisocyanate (IPDI; pure grade, 98%) were purchased from Alfa Aesar (Massachusetts, USA) and used without further purification. Polydimethylsiloxane (PDMS, Mw = 550 g/mol), dibutyltin dilaurate (DBTDL), N-vinyl-2-pyrrolidone (NVP), trimethylolpropane triacrylate (TMPTA), methyl methacrylate (MMA), ethylene carbonate, vinyltrimethoxysilane (VTMS), and poly(ethylene glycol) diacrylate (PEGDA) were purchased from Sigma-Aldrich Inc. (Shanghai, China) and were used as received. Lupranol 1100 (LP1100) was desiccated at 120°C before use, and Laromer 8981 (LR8981) was purchased from BASF. 2-hydroxyethyl methacrylate (HEMA) and tetraethyl orthosilicate (TEOS) were supplied by Merck. Darocur 1173 (DR1173) from Ciba Specialty Chemicals Inc. was used as photoinitiator. *p*-Toluenesulfonic acid (PTSA) was purchased from Fluka. Sodium carbonate, acetone, ethanol, and isopropyl alcohol from commercial sources were used as received. Teflon TM templates (70 mm × 50 mm × 1 mm) were used for free film applications. The UV lamp (Ultrawit 300) was purchased from Osram. Plexiglas test panels (70 mm × 70 mm × 1 mm) purchased from local vendors were used as substrates for all coatings.

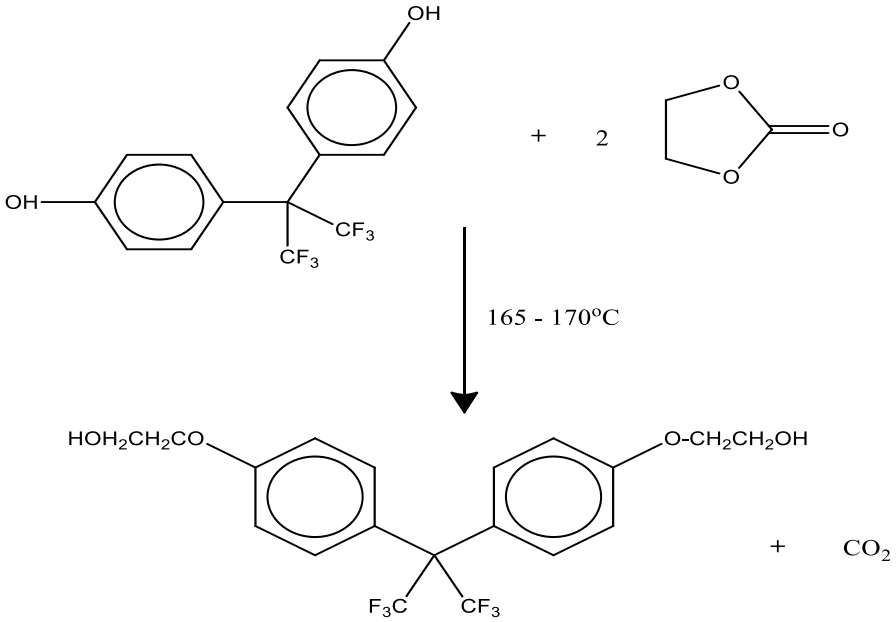

Scheme 1 Synthesis of 2,2-bis(4-β-hydroxyethoxy) phenyl 6F propane (HEPFA)

Methods

Synthesis of 2,2-bis(4-β-hydroxyethoxy) phenyl 6F propane (HEPFA)

HEPFA monomer was obtained from the reaction between ethylene carbonate and BP-AF according to the literature [19]. 0.14 mol (47.55 g) BP-AF, 0.28 mol (24.90 g) ethylene carbonate and 0.07 g sodium carbonate (as catalyst) were charged into a 500-ml round-bottom flask equipped with a mechanical stirrer, a reflux condenser, and a nitrogen inlet. The reaction mixture was then gradually heated to 165–170 °C under nitrogen supply, and the reaction was completed after 4 h. The obtained amorphous compound was washed several times with distilled water to remove the unreacted ethylene carbonate and then dried in a vacuum oven. The chemical structure of HEPFA was determined by FT-IR. The reaction yield was calculated to be 90%. The synthetic pathway of HEPFA is shown in Scheme 1.

FT-IR (cm^{-1}): 3305 (C–OH), 3010 (aromatic C–H), 1614 (aromatic –C=C–), 1240 (aryl–alkyl ether C–O–C), 1130 (C–F).

Synthesis of polyurethane acrylate (PUA) oligomer

Five different UV-PUA oligomers (B, H:20, H:40, P:10/H:20, and P:20/H:40) were synthesized by using different amounts of polyols (HEPFA, LP1100, PDMS), IPDI and HEMA. The abbreviations for the PUAs are as follows: B stands for base polyurethane acrylate (basecoat) without HEPFA and PDMS; H:20/H:40 and P:10/P:20

stand for HEPFA and PDMS, respectively. The numbers represent the weight percentages (wt%) of HEPFA and PDMS content in the base polyurethane oligomers. The compositions of the PUA oligomers are listed in Table 1.

Each PUA oligomer was synthesized in two steps. In the first step, various amounts of polyol LP 1100, HEPFA, and PDMS were added to a three-neck flask equipped with a mechanical stirrer, a dropping funnel, a nitrogen gas inlet, and a condenser. Then, IPDI was added dropwise to the flask to obtain a –NCO terminated prepolymer. During the reaction, DBTDL was used as a catalyst, and the temperature was gradually increased to 60 °C within one hour. The reactants were diluted with a small amount of acetone to adjust the viscosity of the reaction mixture. In the second step, HEMA was added to the reaction mixture within 30 min (–NCO terminated oligomer). Then, the temperature was gradually increased to 50 °C. The reaction was continued until the –NCO band at 2269 cm^{-1} completely disappeared from the spectra of FT-IR. The final product was dried in vacuo at room temperature to evaporate acetone. The synthetic routes of the reactions are shown in Scheme 2. The chemical structures of the PUA oligomers (B, H40, and P20/H40) were determined by FT-IR and ^{1}H-NMR, and the results in brief are given below.

B; FT-IR (cm^{-1}): 3340 (–NH), 2970–2865 (–CH), 1712 (–C=O urethane), 1632 (–C=C– acrylate), 1523 (amide II), 1091 (–C–O–C), 816 (=CH– acrylate).

B; ^{1}H-NMR; (CD_3COCD_3) δ (ppm): 6.36 (IPDI–CH–N<u>H</u>COO), 5.88 (IPDI–CH_2–N<u>H</u>COO–), 6.54–6.03 and 5.73–5.54 (C<u>H</u>$_2$=C– acrylate), 4.40–4.11 (–C<u>H</u>$_2$ of PPG and COOC<u>H</u>$_2$C<u>H</u>$_2$– of HEMA), (3.68–3.27 (–C<u>H</u>$_2$; –C<u>H</u> of PPG and –C<u>H</u> of IPDI), 2.90 (–C<u>H</u>$_2$–NH–COO–), 1.91 (–C<u>H</u>$_3$ of HEMA), 1.11–0.92 (–C<u>H</u>$_2$ of IPDI, –C<u>H</u>$_3$ of IPDI and –C<u>H</u>$_3$ of PPG).

H:40; FT-IR (cm^{-1}): 3358 (–NH), 2972 (–CH), 1710 (–C=O urethane), 1613 (–C=C–, aromatic), 1171 ($-CF_3$).

H:40; ^{1}H-NMR; (CD_3COCD_3) δ (ppm): 7.48–6.85 (<u>H</u>C=C–, aromatic), 6.37 and 5.91 (–CH–N<u>H</u>COO and CH_2N<u>H</u>COO–), 5.91 (IPDI–CH_2–N<u>H</u>COO–), 6.26–6.05 and 5.73–5.54 (C<u>H</u>$_2$=C– acrylate), 4.46–4.15 (–OC<u>H</u>$_2$C<u>H</u>$_2$OCONH– of HEPFA and –COOC<u>H</u>$_2$C<u>H</u>$_2$– of HEMA), 3.86–3.28 (–C<u>H</u>$_2$, –C<u>H</u> of PPG and –C<u>H</u> of IPDI), 2.95–2.82 (–C<u>H</u>$_2$–NHCOO–), 1.91 (–C=C(C<u>H</u>$_3$), 1.78–1.52 (–C<u>H</u>$_2$, cycloaliphatic), 1.37–0.76 (–C<u>H</u>$_3$, IPDI and PPG).

P:20/H:40; FT-IR (cm^{-1}): 3367 (–NH), 2903 (–CH), 1711 (–C=O urethane), 1620 (–C=C–, aromatic), 1171 ($-CF_3$), 811 (Si–CH_3).

Table 1 Contents of UV-curable polyurethane acrylate oligomers (PUAs)

PUA oligomers	LP1100 *g*	HEPFA *g*	PDMS *g*	IPDI *g*	HEMA *g*	HEPFA wt%	PDMS wt%
B	33	–	–	13.34	7.8	–	–
H:20	33	3.18	–	16.67	9.76	20	–
H:40	24.75	6.36	–	16.67	9.76	40	–
P:10/H:20	29.15	3.18	2.06	16.67	9.76	20	10
P:20/H:40	16.5	6.36	4.12	16.67	9.76	40	20

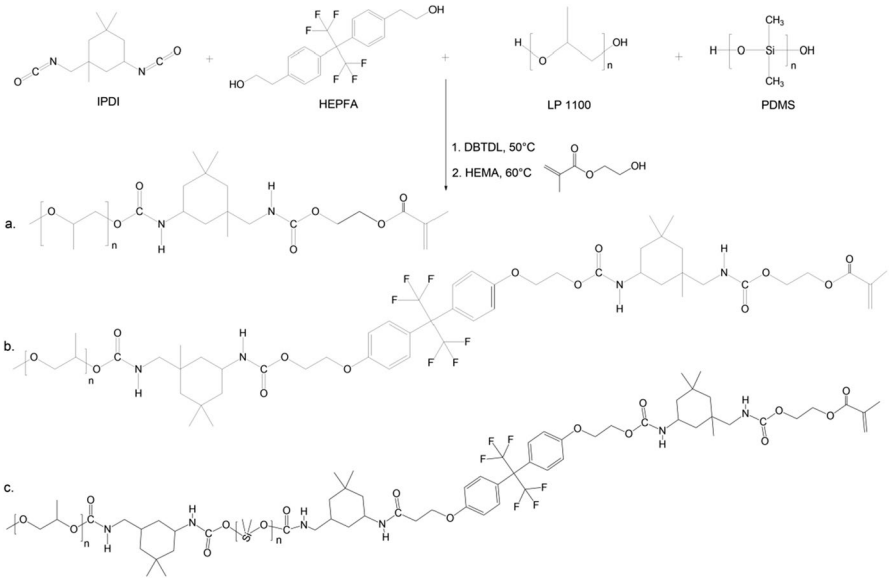

Scheme 2 Synthesis pathways of polyurethane acrylate oligomers; **a** Base PUA (B-PUA); **b** PUA containing HEPFA (H:20 and H:40); **c** PUA containing HEPFA and PDMS (P:10/H:20 and P:20/H:40)

P:20/H:40; ^{1}H-NMR; (CD_3COCD_3) δ (ppm): 7.36–6.74 (HC=C–, aromatic), 6.32 (IPDI–CH–NHCOO), 5.85 (IPDI–CH_2–NHCOO–), 6.06–5.93 and 5.59–5.43 (CH_2=C– acrylate), 4.40–4.03 (–OCH_2CH_2– of HEPFA and 4.20–4.12 –COOCH_2CH_2– of HEMA), 3.75–3.60 (–OCHCH_3, PPG), 3.56–3.19 (–CH–NHCOO of IPDI), 2.95–2.72 (–CH_2–NHCOO–), 1.81 (–C=C(CH_3), 1.70–1.42(–CH_2, cycloaliphatic), 1.31–0.66 (–CH_3, IPDI and PPG), 0.03 (–Si–CH_3, PDMS).

Synthesis of the sol–gel precursor

The silica precursor solution was prepared by adding 0.045 mol (9.41 g) TEOS, 0.0225 mol (3.349 g) VTMS, 0.1575 mol (3.236 g) deionized water, and 0.1085 mol (5 g) ethanol to an amber glass bottle at room temperature. Then, 0.1 g of PTSA was added as a catalyst. The pH of the reaction mixture was maintained at 3 to 4 by the content of PTSA. The reaction mixture was magnetically stirred at room temperature for 24 h, and the partially hydrolyzed sol–gel solution was obtained.

Preparation of the UV-cured PUA hybrid coating materials

The different formulations of UV-curable PUAs and nano-hybrid materials were prepared as follows: PUA oligomers were mixed with LR8981, NVP, PEGDA, TMPTA, MMA, and Darocur 1173 in a 10 ml beaker. Then, the different amounts of sol–gel solution were added to the mixture and stirred until a clear, homogeneous form was obtained. Finally, the UV-curable PUA hybrid coating formulations

were cast onto Plexiglas panels (70 mm × 70 mm × 1 mm) using a wire-gauged bar applicator, achieving a film thickness of about 30 µm. The Plexiglas panels were cleaned with isopropyl alcohol after removing the protective film, and the Plexiglas surfaces were subjected to oxygen plasma treatment using Ugur Electronic *D*-600 Corona Generator with a power of 1.5 kW before the coating process. In this case, the adhesion between the Plexiglas panels and the coating materials was increased. In addition, the free films were prepared by filling the formulations into Teflon wells (10 mm × 5 mm × 1 mm). Then, all formulations were cured with an Osram VITALUS 300 W UV lamp for 3 min. The compositions of the hybrid formulations are listed in Table 2. In addition, the synthesis route of the UV-cured hybrid coating materials is shown in Scheme 3.

Characterization

Fourier transform infrared spectroscopy (FT-IR) (PerkinElmer ATR FT-IR spectrophotometer) and ^{1}H NMR were used to study the chemical structure of the monomers and polyurethane acrylate oligomers. All FT-IR spectra were scanned in the

Table 2 Compositions of UV-curable hybrid polyurethanes

Formulations*	B (wt%)	H:20 (wt%)	H:40 (wt%)	P10:H20 (wt%)	P20:H40 (wt%)	Sol–gel (wt%)
B	50	–	–	–	–	–
B/S10	50	–	–	–	–	10
B/S20	50	–	–	–	–	20
B/S30	50	–	–	–	–	30
H20	–	50	–	–	–	–
H20/S10	–	50	–	–	–	10
H20/S20	–	50	–	–	–	20
H20/S30	–	50	–	–	–	30
H40	–	–	50	–	–	–
H40/S10	–	–	50	–	–	10
H40/S20	–	–	50	–	–	20
H40/S30	–	–	50	–	–	30
P10:H20	–	–	–	50	–	–
P10:H20/S10	–	–	–	50	–	10
P10:H20/S20	–	–	–	50	–	20
P10:H20/S30	–	–	–	50	–	30
P20:H40	–	–	–	–	50	–
P20:H40/S10	–	–	–	–	50	10
P20:H40/S20	–	–	–	–	50	20
P20:H40/S30	–	–	–	–	50	30

*All formulations containing same amount of reactive diluents to support crosslinking of the UV curable groups; TMPTA (15 wt%), LR8981 (10 wt%), MMA (5 wt%), NVP (5 wt%), PEGDA (12 wt%), Darocur1173 (3 wt%). The sol–gel solution was calculated based on the total resin weight

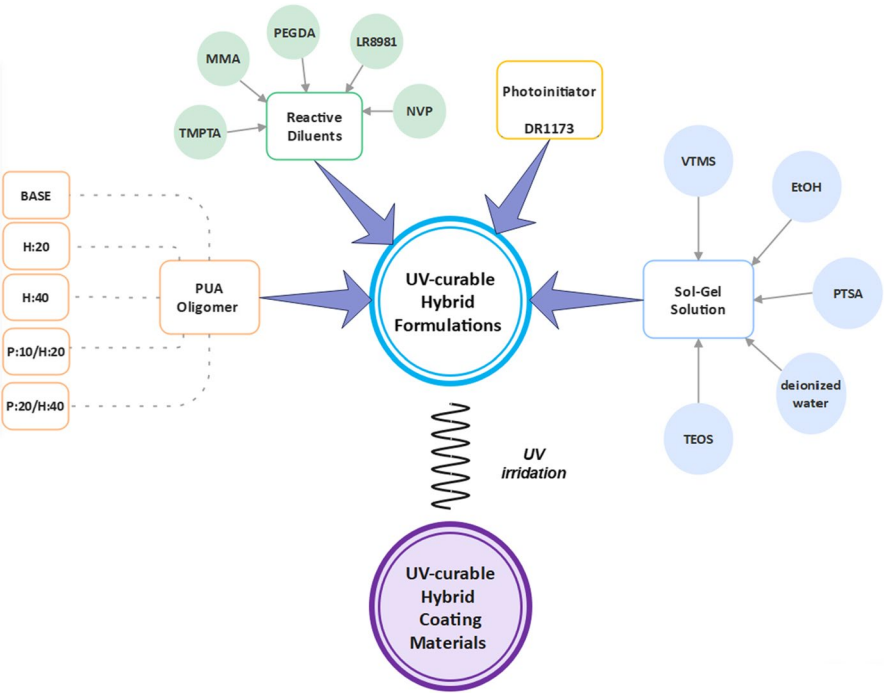

Scheme 3 Flowchart of UV-cured hybrid coating materials

range of 400–4000 cm^{-1}. The ^{1}H NMR analysis of the PUAs in CD_3COCD_3 was recorded using a Varian VX400 BB model NMR spectrometer.

Gloss values of the coated panels were determined using a BYK-Gardner Micro-TRI glossmeter at 20° and 60° according to ASTM D-523-80.

Cross-cut test results were determined using the P-A-T Paint Adhesion Test Kit according to DIN 53151.

The hardness of the coatings was measured using the BYK-Gardner pendulum hardness tester (König/Persoz) according to ASTM D 4366.

The water absorption values were calculated as follows: The UV-cured PUAs and nano-hybrid films were cut into pieces and dried in a vacuum oven for one day to determine their dry weight (m_1). Then, they were soaked in distilled water for 48 h at room temperature. The swollen samples were blotted with filter paper and weighed (m_2). Water absorption values were determined using an average of five measurements. The water absorption values (w) of the formulations were calculated using the following equation:

$$w\,(\%) = \frac{m_2 - m_1}{m_1} \times 100 \tag{1}$$

$$A\,(\%) = \frac{w_2}{w_1} \times 100 \tag{2}$$

The gel contents of the UV-cured hybrid films were carried out by the Soxhlet extraction method using acetone for 6 h. The gel content ratio was calculated by the following equation, where w_1 and w_2 are weights of the samples before and after the extraction, respectively.

The wettability properties were evaluated by the contact angle (θ) of the PUA hybrid films. The contact angles of the films with deionized water and ethylene glycol were determined at room temperature using a Kruess tensiometer (Easy Drop DSA-2) by the sessile drop test method. The contact angle results were obtained with an average of five measurements at different points on the surface of the Plexiglas-coated hybrid resin.

The thermogravimetric behavior of the UV-cured hybrid films was recorded using a PerkinElmer Pyris 1 TGA Tg analyzer. The films were placed in a ceramic pan and heated from 30 to 750 °C at a fixed heating rate of 10 °C/min under an air atmosphere.

The flame retardancy of the PUA and nano-hybrid films was analyzed by the limiting oxygen index (LOI) method using the Fire Testing Technology Instrument according to ASTM D 2863.

The surface morphology of the UV-cured PUA hybrid films was examined using SUPRA 35 VP, LEO scanning electron microscopy (SEM). Prior to scanning, the coating films were freeze-fractured in liquid nitrogen and then coated with a thin gold layer of approximately 300 Å.

The UV–visible spectra of the PUA hybrid films were observed in the range of 200–800 nm using a Shimadzu UV 6010 spectrophotometer.

Mechanical properties of the PUA hybrid films were determined by standard tensile stress–strain tests to measure the modulus (E), ultimate tensile strength (δ) and elongation at break (ε) using a Zwick Roell 500 N testing machine with an initial force of 5 N and an under 3 mm/min elongation rate. The results were the average values of five tests.

Results and discussion

The objective of this study was to develop a series of UV-curable fluorine—and silicone—containing polyurethane-based hybrid coating materials by the sol–gel method and to investigate the effects of HEPFA, PDMS and sol–gel contents on coating properties.

Structural characterization of HEPFA and PUA oligomers

A fluorine-containing diol compound (HEPFA) was prepared by the reaction of bisphenol-AF and ethylene carbonate, given in Scheme 1. Figure 1 shows the FT-IR spectrum of HEPFA. The peaks originated from the functional groups of HEPFA are as follows: HEPFA showed a characteristic broadband at 3305 cm^{-1}, which was

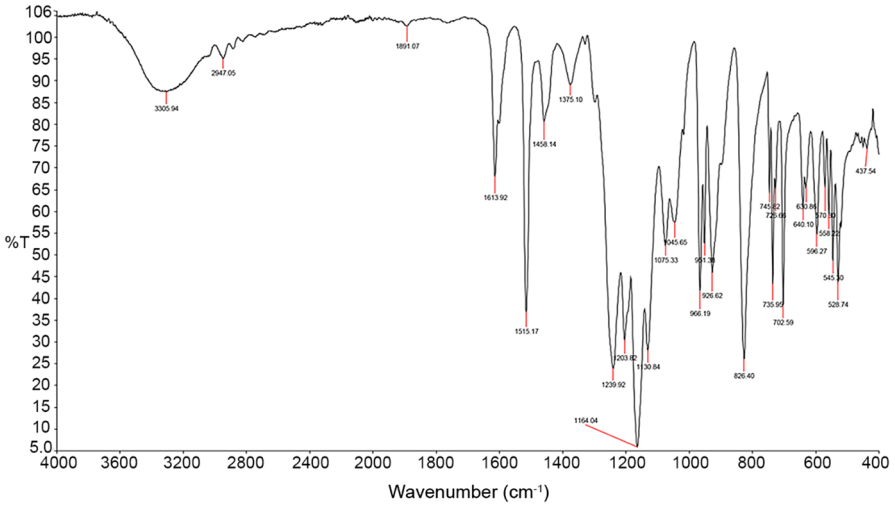

Fig. 1 FT-IR spectrum of 2,2-bis(4-β-hydroxyethoxy) phenyl 6F propane (HEPFA)

due to the O–H group. The symmetric C–O–Ar stretching vibration of the alkyl aryl ether was found at 1240 cm^{-1}. The C–F stretching vibration of the alkyl halide was found at 1130 cm^{-1}. These peaks confirm the structure of HEPFA.

Different amounts of LP1100, HEPFA, and PDMS were used for the synthesis of PUA oligomers (B, H20, H40, P10:H20, P20:H40), as shown in Table 1. In addition, the synthetic routes were described in Scheme 2. The FT-IR spectrum B PUA oligomer is shown in Fig. 2. The disappearance of the –NCO band at 2264 cm^{-1} and the formation of the broad N–H band at 3340 cm^{-1} were monitored in the FT-IR spectrum recorded during the PUA synthesis. The absence of the –NCO peak indicates that the –NCO terminated prepolymer reacted with the –OH groups of HEMA. Moreover, the aliphatic C–H stretching vibrations (symmetric and asymmetric) of PPG (LP1100) were observed in the range of 2970–2865 cm^{-1}. The sharp absorption band of the C=O stretching vibration is detected at 1712 cm^{-1}, indicating the presence of the carbonyl group in the urethane structure. The C–O–C stretching vibrations at 1091 and 1164 cm^{-1} belong to the carbamate structure and HEMA, respectively. The absorption bands of the acrylate group were recorded at 1632 and 816 cm^{-1} for C=C stretching vibrations and =C–H bending vibrations, respectively. The amide-II band formed by the combination of N–H bending vibration and C–N stretching vibration was observed at 1523 cm^{-1}.

Figure 3 shows the ^{1}H NMR spectrum of the base polyurethane acrylate (B) in acetone-d6. The peaks belong to the $–CH_3$ protons of PPG, IPDI, and the cycloaliphatic –CH2 protons of IPDI in the range of 1.11–0.92 ppm. At 1.95 ppm, the $–CH_3$ protons of HEMA are identified. The $–CH_2$ protons of IPDI bonded to the urethane nitrogen atom are detected at 2.90 ppm. The –CH, $–CH_2$ protons of PPG and the –CH protons of IPDI are detected at 3.68–3.27 ppm. The $–CH_2$ protons attached to the oxygen of the ester group of HEMA ($–COOCH_2CH_2$) are recorded at 4.40–4.11 ppm. The peaks in the 6.54–6.03 and 5.73–5.54 ppm ranges belong

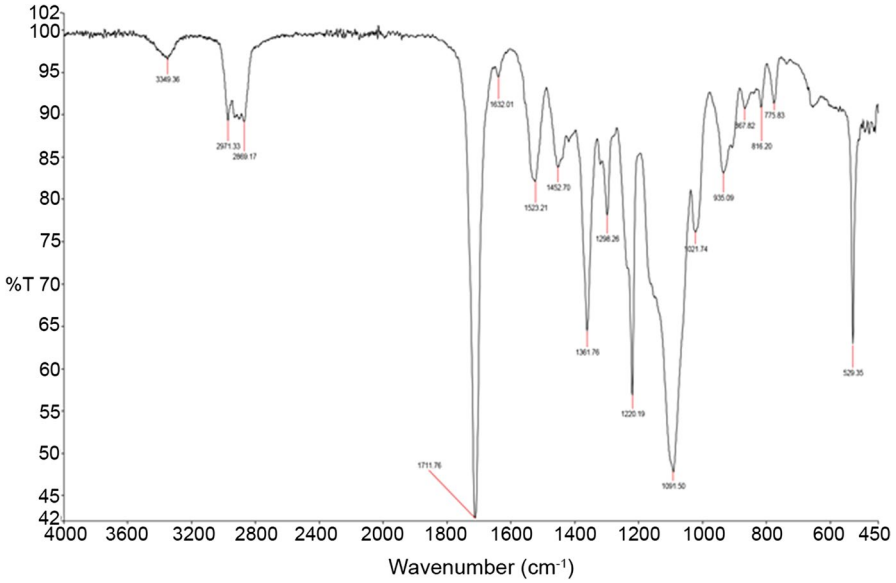

Fig. 2 FT-IR spectrum of the base UV-curable polyurethane acrylate (B)

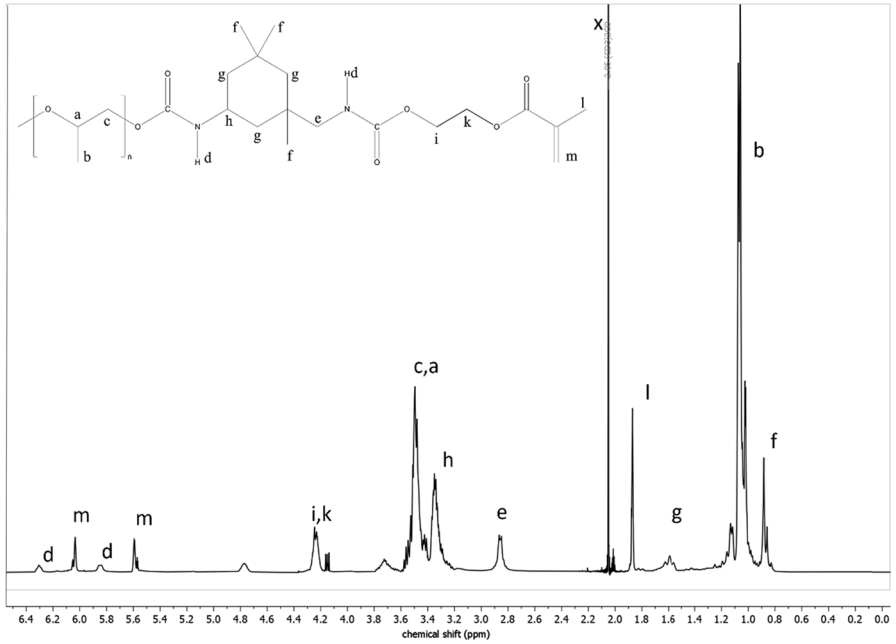

Fig. 3 [1]H-NMR spectrum of the base UV-curable polyurethane acrylate (B)

to the acrylic $–CH_2$ protons ($–CH_2=C$). The –NH protons in the urethane group are observed at 6.36 and 5.88 ppm. The FT-IR and ^1H NMR results are in good agreement with the expected compound.

Figures 4 and 5 show the FT-IR spectra of PUA with HEPFA (H:40) and PUA with PDMS and HEPFA (P:20/H:40), respectively. The absence of the –NCO band shows that the –OH group of HEMA successfully reacted with the –NCO group of IPDI in both spectra. All the characteristic peaks of a typical polyurethane were detected in the spectra of H:40 and P:20/H:40 as follows: The formation of the broad N–H band (N–H stretching vibration) of the urethane linkage was observed at 3358 cm^{-1} for H:40 and 3367 cm^{-1} for P:20/H:40. The aliphatic-CH_2 stretching vibrations (asymmetric and symmetric) of H:40 and P:20/H:40 were recorded at 2972 and 2903 cm^{-1}, respectively. The C=O and C–O–C stretching vibrations of the urethane group were recorded at about 1711 and 1092 cm^{-1} for H:40 and P:20/H:40 oligomers, respectively. The C=C stretching of benzene ring in HEPFA structure was recorded at 1613 cm^{-1} for H:40 and P:20/H:40. The 6F group of HEPFA was observed at 1171 cm^{-1}. The presence of these bands indicates that the HEPFA monomer successfully reacted with other monomers in the formation of the polyurethane. Additionally, the.

P:20/H:40 oligomer showed a stretching band at 811 cm^{-1} associated with the Si-CH_3 bond, confirming the presence of PDMS in the polyurethane resin.

The ^1H NMR spectrum provides more precise information about the structure of the synthesized PUA oligomers. The ^1H NMR spectrum of the H:40 in CD_3COCD_3 is shown in Fig. 6**,** and the corresponding protons are as follows: The $–CH_3$ protons of IPDI and PPG are recorded in the range of 1.37–0.76 ppm. The cycloaliphatic $–CH_2$ protons of IPDI and the $–CH_3$ protons of HEMA are recorded at 1.78–1.52

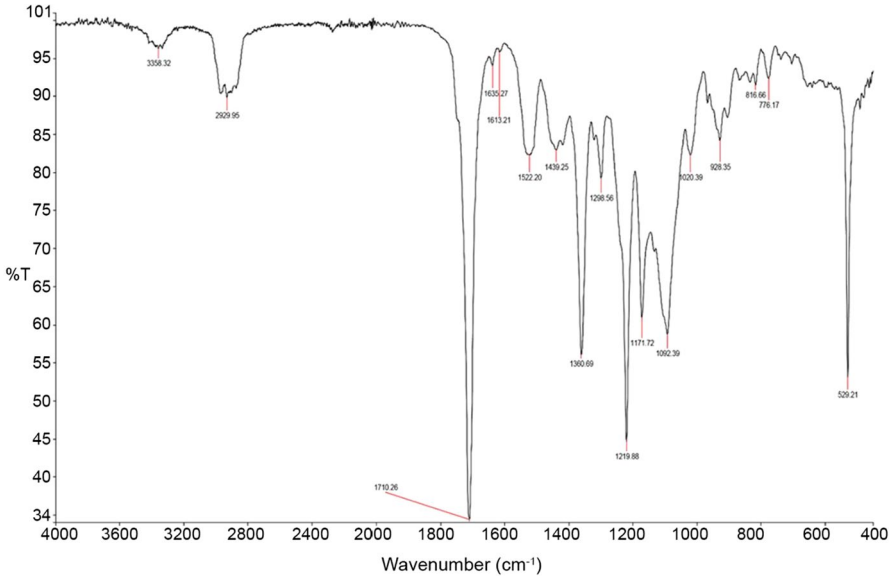

Fig. 4 FT-IR spectrum of the polyurethane acrylate containing HEPFA (H:40)

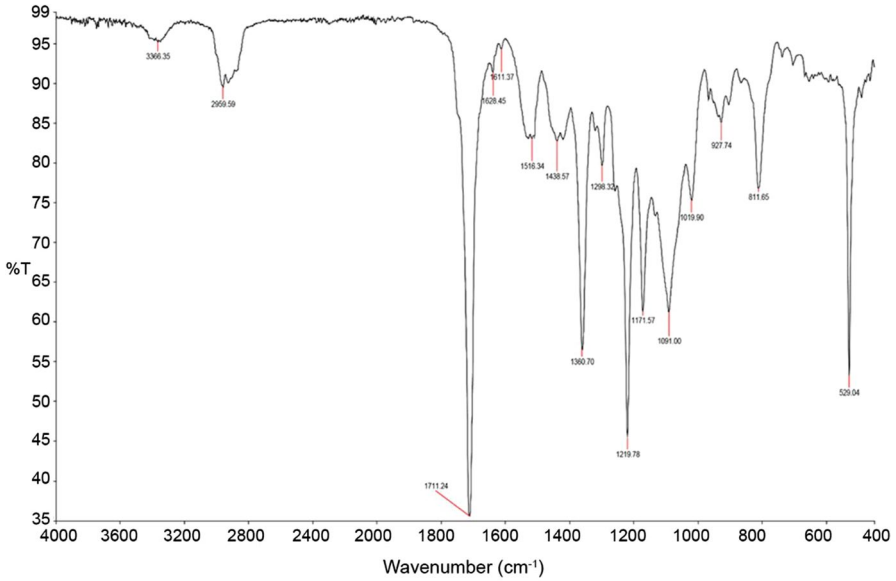

Fig. 5 FT-IR spectrum of the polyurethane acrylate containing HEPFA and PDMS (P:20/H:40)

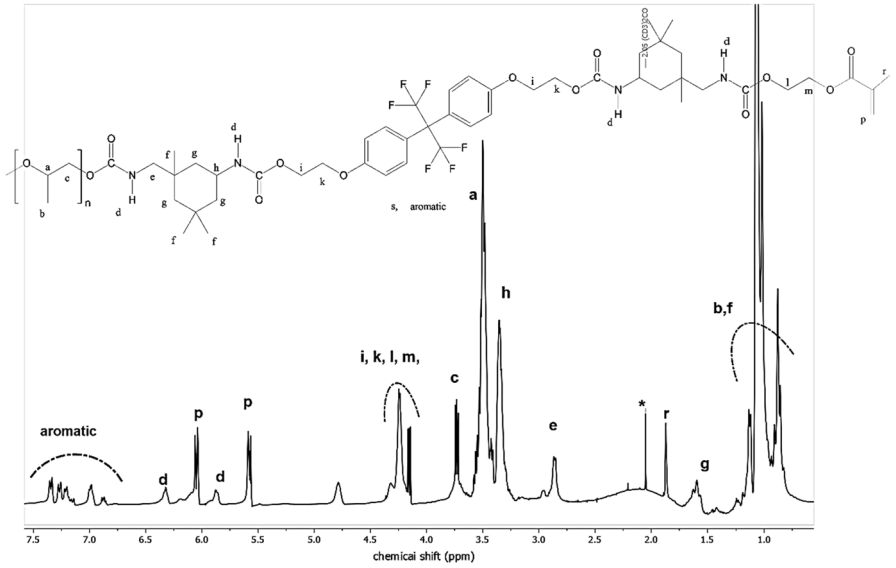

Fig. 6 [1]H-NMR spectrum of the H:40 oligomer

and 1.91 ppm, respectively. The $–CH_2$ protons attached to the nitrogen atom of the urethane group are detected at 2.95–2.82 ppm. The –CH, $–CH_2$ protons of PPG, and the –CH protons of IPDI were recorded at 3.86–3.28 ppm. The $–CH_2$ protons

of HEPFA (OCH_2CH_2OCONH–) and HEMA (–$COOCH_2CH_2$–) are detected in the range of 4.46–4.15 ppm. The acrylic –CH_2 protons (–CH_2=C–) of HEMA are recorded in the range of 5.73–5.54 and 6.26–6.05 ppm, respectively. The –NH protons of urethane groups are observed at 5.91 ppm (–CH_2NHCOO–) and 6.37 ppm (–CH–NHCOO). The aromatic protons of HEPFA were measured to range between 7.48 and 6.85 ppm. The results indicate that the oligomer H40 was successfully synthesized.

Figure 7 shows the ^{1}H-NMR spectrum (CD_3COCD_3) of the P20:H40 oligomer. The chemical shifts of the protons were as follows: The Si-CH_3 proton signals of PDMS are at 0.03 ppm. The protons of –CH_3 in IPDI and PPG were recorded at 1.36–0.66 ppm. The –CH_2 protons in the cyclic ring of IPDI were recorded at 1.70–1.42 ppm. The –CH_3 protons of HEMA and the –CH_2 protons bound to the nitrogen atom of IPDI are determined at 1.81 ppm and 2.95–2.72 ppm, respectively. In addition, the –CH, –CH_2 protons of PPG and the –CH protons of IPDI at 3.75–3.19 ppm, the protons of HEPFA (OCH_2CH_2OCONH–) and HEMA (–$COOCH_2CH_2$–) at 4.40–4.12 ppm, the acrylate protons (–CH_2=C–) of HEMA at 6.06–5.93 and 5.59–5.43 ppm, the –NH groups in the urethane structure at 6.32 and 5.85 ppm and the aromatic protons in HEPFA at 7.36–6.74 ppm were also determined. These results prove that the P20:H40 oligomer was successfully obtained.

Physical properties

The physical properties of the hybrid coatings, such as pendulum hardness, cross-cut adhesion, gloss, gel content, and water absorption, are shown in Table 3.

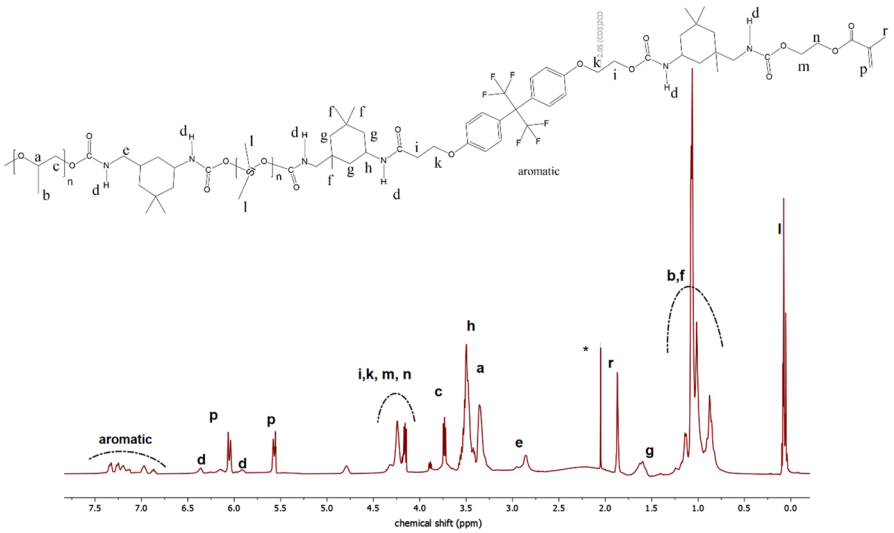

Fig. 7 ^{1}H-NMR spectrum of the P:20/H:40 oligomer

Table 3 Physical properties of UV-cured PUA coatings

Formulations	Gel content (wt%)	Cross-cut adhesion	Pendulum hardness (König)	Water-absorption (wt%)	Gloss 20°	60°
B	96	0	83.7	4.7	98	136
B/S10	96.4	0	97.7	4.4	101	128
B/S20	96.9	0	109.7	4.3	127	147
B/S30	97.2	0	113.5	4.1	129	141
H20	98.1	0	102	4.4	108	133
H20/S10	98.4	0	111.7	4.1	115	134
H20/S20	98.7	0	111.3	3.8	121	131
H20/S30	99.1	0	115.3	3.5	128	109
H40	98.2	0	113	4.2	117	130
H40/S10	98.7	0	116.5	3.7	123	136
H40/S20	99.3	0	117	3.4	126	136
H40/S30	99.4	0	119.6	3	130	137
P10:H20	98.6	0	111.5	3.5	122	135
P10:H20/S10	99.4	0	113.8	3.3	125	136
P10:H20/S20	99.4	0	116.7	3.2	129	141
P10:H20/S30	99.5	0	118.3	2.8	136	142
P20:H40	98.9	0	118.6	3.2	133	142
P20:H40/S10	99.4	0	121	2.9	128	133
P20:H40/S20	99.3	0	121.6	2.6	133	140
P20:H40/S30	99.6	0	123.6	2.5	137	142

Gloss

Gloss is an important feature for the coating industry which depends on the interaction of light with the physical properties of the coating surface; it is determined using a glossmeter, which projects light at specific angles onto the coating surface and simultaneously measures the amount of reflected light. Depending on the gloss level of the surface, different angles can be selected for the light, e.g., 20° for high-gloss surfaces, 60° for semi-gloss surfaces, and 85° for low-gloss surfaces. All the UV-cured PUA coatings on Plexiglas panels were measured at angles of 20°, 60°, and 85°. However, due to the high-gloss properties of the coating materials, only the results at 20° and 60° were listed in Table 3. When the amount of HEPFA in the base urethane acrylate was increased from 0 wt% to 20 and 40 wt%, the gloss values at 20° were also increased from 98° to 108° and 117° for H20 and H40 PUA, respectively. Addition of the PDMS structure in the B oligomer increased the gloss values from 98° to 122° for P10:H20 and 133° for P20:H40 formulations. The hybrid coatings exhibited better gloss compared to the pure PUA coatings. Moreover, the gloss values of the coatings gradually increased with increasing sol–gel content. This could be attributed to the more effective crosslinking and higher silicate and fluorine functionality, resulting in a more uniform film surface.

Cross-cut adhesion

The adhesion between the Plexiglas panels and the coating formulations was investigated by a cross-cut adhesion test according to the standard DIN 53151. The classification of adhesion, based on the percentage of area removed, ranges from 0 to 5, with 0 representing excellent adhesion and 5 representing poor adhesion. All coating materials showed excellent adhesion properties, as can be seen in Table 3. The data can be attributed to the perfect interaction between the urethane acrylate oligomers and Plexiglas surfaces. These results are also supported by the gel content of the coating materials.

Gel content

The gel content is determined by Soxhlet extraction, which is used to calculate the insoluble fractions of the crosslinked or network polymers. The data presented in Table 3 show that the values of the gel content of the films ranged from 96.0 to 99.6%. These results can be attributed to the high crosslinking rate and good degree of cure of the films. In addition, this promoted increasing density and photosensitive group content in UV-curable PUA resins, which was also supported crosslinking and improved film performance.

Water absorption

The samples were tested for water resistance as shown in Table 3, and all coatings showed a decrease in water absorption compared to the urethane basecoat (B). The nano-hybrid coatings also showed lower water absorption than neat PUA coatings, which changed dramatically as the amount of sol–gel precursor increased. This could be due to the increase in the crosslink density of the siloxane network in the polyurethane matrix [21]. When comparing the urethane–acrylate coatings (B, H20, H40, P10:H20, P20:H40) with each other, the water absorption also decreased as HEPFA and PDMS increased. The water absorption of B decreased from 4.7 wt% to 4.4 and 4.2 wt% for H20 and H40, respectively, when the HEPFA content in the PUA was increased from 20 to 40 wt%. In this context, the P20:H40 formulation showed the best water resistance compared to other urethane acrylates. This can be attributed to the hydrophobic nature of HEPFA which contains rigid aromatic and fluorine groups, and PDMS which tends to accumulate on the coating surface, preventing water molecules from dissolving the coatings [30, 37].

Pendulum hardness

Pendulum hardness test is a damping method evaluated by the loss of kinetic energy of the tool on the surface of sample. The energy loss is converted into a hardness value that in accordance with standards. The procedure as König is based on the concept of friction. The softer the coating, the shorter the time required for an oscillating pendulum. As shown in Table 3, the hardness of the PUA coatings enhanced significantly with increasing amounts of HEPFA compared to the urethane basecoat

(B). The hardness of B increased from 84 to 102 and 113 for H20 and H40, respectively. This can be attributed to the rigid aromatic groups of HEPFA, which increase the stiffness of the polymer chains [39]. In the case of incorporation of PDMS in the PUA containing HEPFA, the hardness of P10:H20 and P20:H40 was determined to be 112 and 119, respectively. This result can be ascribed that siloxane bonds in the polymer backbone played a role in slightly improving hardness. In addition, the hardness of all hybrid coatings increased when the sol–gel content was increased. The hardness of the hybrid films gradually increased from 84 to 124 when the sol–gel solution was added to all polyurethane formulations. This can be attributed to the rigidity by the formation of stable and dense Si–O–Si network during the sol–gel process [21].

Contact angle

The contact angle values of polyurethane acrylates and their nano-hybrid coatings were investigated using the sessile drop test method. The contact angle data (CAs°) of the samples with deionized water and ethylene glycol are shown in Table 4. Measurements were taken on the right and left sides of each droplet. The droplets were applied to the Plexiglas covered with the formulations at 5 different locations

Table 4 Contact angle and transmittance values of PUA hybrid coatings

Formulations	Contact angle (θ/°)		Transmittance (%)	
	Deionized water	Ethylene glycol	700 nm	500 nm
B	52	48	100	97.26
B/S10	58	52	100	97.12
B/S20	61	55	99.40	96.48
B/S30	64	57	100	98.23
H20	65	61	99.70	95.98
H20/10	67	63	99.70	97.27
H20/S20	69	66	99.70	96.97
H20/S30	71	69	100	97.70
H40	70	65	99.70	96.20
H40/S10	73	67	99.40	97.20
H40/S20	73	70	99.40	96.20
H40/S30	75	71	99.40	96.90
P10:H20	72	66	99.70	96.30
P10:H20/S10	72	68	99.70	96.70
P10:H20/S20	73	71	100	97.40
P10:H20/S30	75	73	99.50	97.20
P20:40	73	69	99.20	95.23
P20:H40/S10	73	72	98.70	94.76
P20:H40/S20	75	73	99.23	95.70
P20:H40/S30	78	76	100	98.47

and the average values were determined. The contact angle values of deionized water and ethylene glycol for the coating films changed in a range of 52°–78° and 48°–76°, respectively. For the polyurethane coating films containing HEPFA and PDMS, the contact angles of deionized water/ethylene glycol were 52°/48° for B; 65°/62° for H20; 70°/65° for H40; 72°/66° for P10:H20; and 73°/69° for P20:H40. The results showed that the incorporation of HEPFA and PDMS structures into the PU backbone gradually increased the water/ethylene glycol contact angles. Moreover, the hybrid coating formulations with a higher sol–gel content also showed better contact angle values. When 30 wt% of the sol–gel solution was added to the polyurethane formulations, the water/ethylene glycol contact angle values were measured as follows: 64°/57° for B/S30, 71°/69° for H20/S30, and 75°/71° for H40/S30, 75°/73° for P10:H20/S30 and 78°/76° for P20:H40/S30. A number of factors can be attributed to these results, including the increased crosslink density due to the increase in sol–gel content as well as the increased stiffness resulting from PDMS and HEPFA incorporation as well as the good synergistic effects between PUAS and sol–gel precursors. Since these polyurethanes have much lower surface energy than the polyurethanes without HEPFA, PDMS and sol–gel, these groups were expected to migrate to the film surface during film formation and crosslinking, leading to an increase in contact angles. [21, 30, 37].

Thermal properties

The thermal behavior of the hybrid coatings was investigated by TGA in air atmosphere. The TGA thermograms of the films are given in Fig. 8a–e. The thermal degradation values of the hybrid coatings are listed in Table 5. Since the unreacted volatile and semi-volatile organic components (i.e., photo-initiator, monomers, oligomers, residual moisture, etc.) were present in the coating films, all the samples showed a slight weight loss of about 5 wt% between 250 and 280 °C. The first weight loss of the films was observed between 279 and 370 °C, which corresponded to the breaking of the urethane bonds. The second and the last weight loss of the polyurethanes were in the range of 408°–430 °C and 541°–612 °C, respectively. This can be explained by the degradation of the polymer. The results showed that the decomposition temperatures are significantly shifted to higher values with increasing content of HEPFA, PDMS and the sol–gel precursor compared to the urethane basecoat (B). It is well-known that polyols containing aromatic groups exhibit better thermal behavior than aliphatic polyols. The incorporation of HEPFA in the PUA improved the thermal properties of the coatings, as expected due to its aromatic structure containing fluorine groups [33, 34]. In the case of increasing the PDMS and sol–gel content, the improvement in thermal stability can be attributed to the higher dissociation energy of the Si–O bond (110 kcal/mol) compared to C–O (85.5 kcal/mol), C–C (82.6 kcal/mol) and Si–C (76.0 kcal/mol) [3].

The high char yield of the samples could be an advantage for flame retardancy. The char ruins of B, H20, H40, P10:H20 and P20:H40 were determined between 0.06 and 0.71. The results presented in Table 5 show that the char residues increased significantly with increasing HEPFA content in the urethane basecoat (B). However,

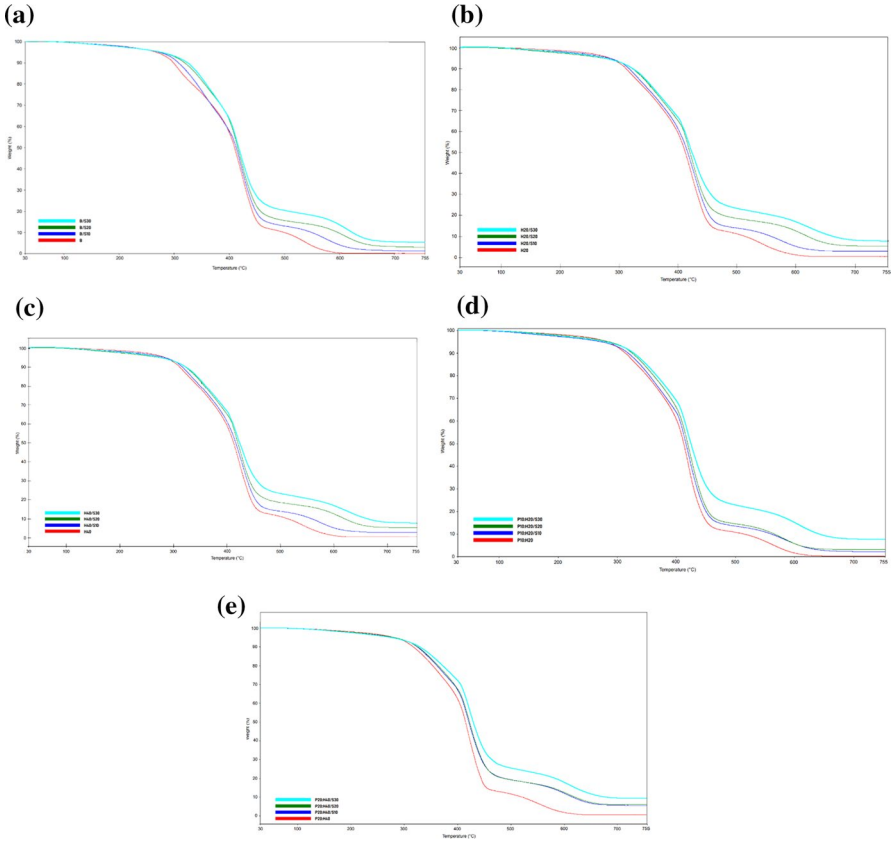

Fig. 8 TGA thermograms of hybrid polyurethanes, **a** B-B/S30, **b** H20-H20/S30, **c** H40-H40/S30, **d** P10:H20-P10:H20/S30, **e** P20:H40-P20:H40/S30

the char ruins increased slightly when PDMS was added to the HEPFA-containing polyurethanes. The char yield of the pure formulations (B, H20, H40, P10:H20 and P20:H40) increased significantly with increasing sol–gel content. It was observed that the char ruins of the hybrids ranged from 1.23 to 9.47 wt%. The results of the limited oxygen index (LOI) results are shown in Table 5. Accordingly, the LOI values of the B and P20:H40/S30 formulations ranged from 18.10 to 20.30 and increased slightly with increasing amounts of HEPFA, PDMS, and sol–gel precursors.

Morphological properties

One of the most important factors affecting the performance and properties of hybrid materials is the quality of dispersion of inorganic nanoparticles in the polymer matrix. Silica particles tend to agglomerate in the polymer matrix due to the hydroxyl groups in their structure. Good dispersion of the particles in the polymer

Table 5 Thermal properties of hybrid coating materials

Samples	First weight loss, (°C)	Second weight loss (50%), (°C)	Last weight loss, (°C)	Char ruins at 750°C, (wt%)	LOI, (%)
B	279	408	541	0.06	18.10
B/S10	288	412	571	1.23	18.40
B/S20	302	415	565	3.03	18.60
B/S30	342	418	579	5.23	18.70
H:20	314	412	542	0.36	18.30
H20/S10	324	416	575	2.30	18.50
H20/S20	343	420	585	5.73	18.60
H20/S30	352	424	609	7.71	18.80
H:40	317	413	543	0.65	18.60
H40/S10	330	420	584	2.83	18.90
H40/S20	345	422	599	5.32	19.10
H40/S30	358	424	619	7.63	19.20
P10:H20	320	413	556	0.37	19.30
P10:H20/S10	340	416	585	3.14	19.50
P10:H20/S20	352	419	587	5.82	19.80
P10:H20/S30	368	425	607	8.01	20.10
P20:H40	330	415	560	0.71	19.40
P20:H40/S10	343	421	607	3.62	19.70
P20:H40/S20	349	422	608	6.11	20.10
P20:H40/S30	370	429	612	9.02	20.30

matrix can be achieved either by surface modification of the silica or by in situ polymerization methods. The dispersion of nanoparticles is based on the compatibility between the sol–gel mixture and the organic matrix. In this study, the compatibility between the polyurethane phase and the inorganic phase was achieved by using vinyl-3-methoxysilane (VTMS). In addition, the hybrid formulations ultrasonically stirred to prevent the agglomeration of silica particles. The morphology of the PUA coatings and their nano-hybrids was investigated by SEM. The microscopic images of the fractured surfaces of the films are shown in Fig. 9a–f. Figure 9a–c shows the SEM microscopic images of B, H40 and P20:H40 polyurethane coatings, respectively. The image of formulation B was homogeneous. When HEPFA and PDMS were incorporated into the PUA backbone, H40 and P20:H40 were also homogeneous. A possible explanation for this is that HEPFA and PDMS compounds do not cause phase separation in the PUAs. Moreover, when the 30 wt% sol–gel solution was incorporated into the B, H40 and P20:H40 polyurethanes, it was observed that the nano-silica particles were scattered in the polymer matrix without serious agglomeration (Fig. 9d–f). As can be seen from the images of B/S30, H40/S30 and P20:H40/S30, the spherical silica nanoparticles had a very small size ranging from 30 to 73 nm and s showed homogeneous morphology. This could be due to the good chemical interactions between the sol–gel precursors and PUAs.

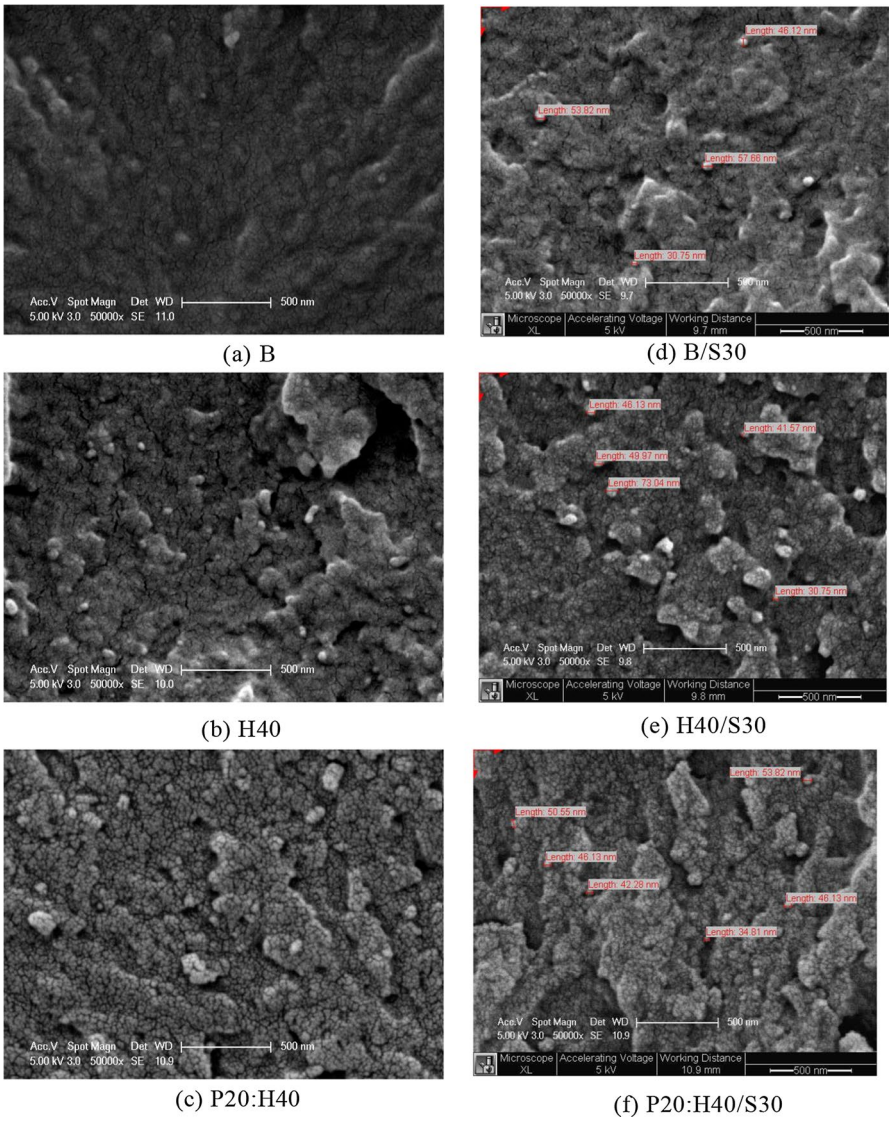

Fig. 9 SEM images of polyurethanes at 500 nm; **a** B, **b** H40, **c** P20:H40, **d** B/S30, **e** H40/S30 **f** P20:H40/S30

Optical transparency of the hybrid coatings

The optical transparencies of the hybrid coatings were investigated using a UV–visible spectrophotometer. The UV–visible spectra of the cured films are shown in Fig. 10a–e. The transmittance values of the spectra at 700 nm and 500 nm are also listed in Table 4. As can be seen in the figures, neither the addition of HEPFA and PDMS compounds nor the addition of the sol–gel solution led to a significant

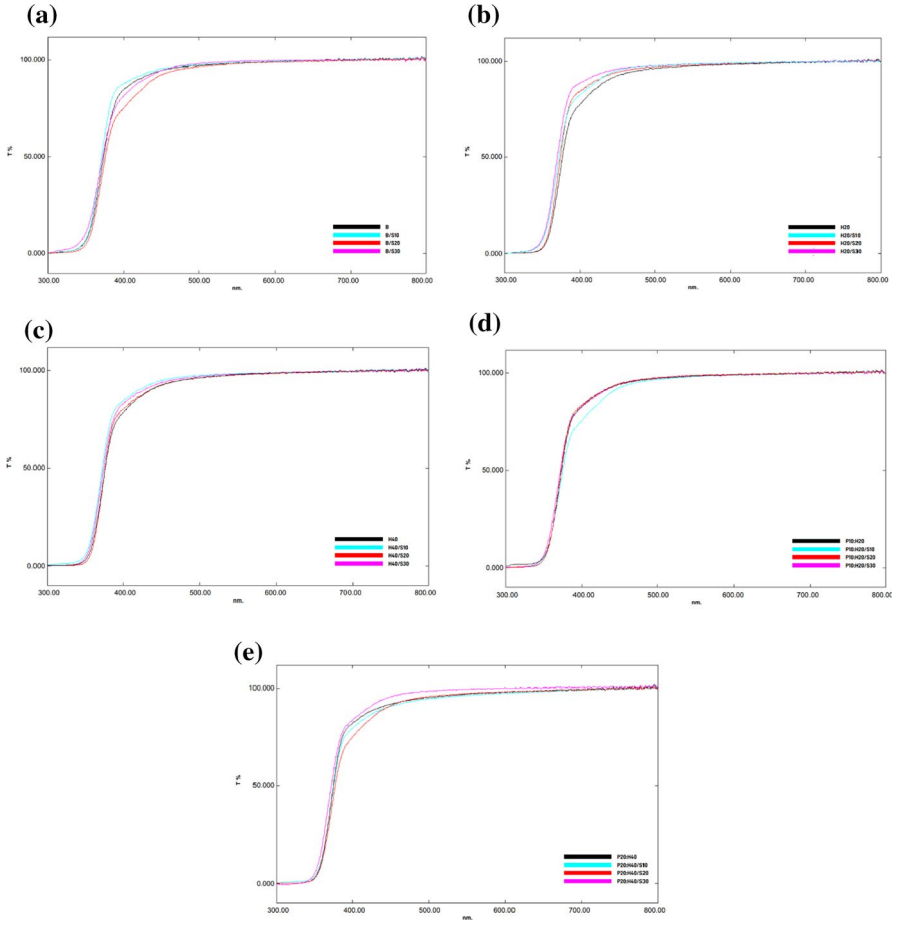

Fig. 10 UV–visible spectrums of UV-cured polyurethane coatings. **a** B-B/S30, **b** H20-H20/S30, **c** H40-H40/S30, **d** P10:H20-P10:H20/S30, **e** P20:H40-P20:H40/S30

decrease in the optical transmittance of the B polyurethane. These results can be attributed to the fact that there was no phase separation between the organic and inorganic phases, and there was good compatibility. It can be concluded that all the coating films have good optical transparencies in the visible range.

Mechanical properties

Table 6 lists the mechanical properties of all the coating films, such as tensile modulus (E), tensile strength (r) and elongation at break (E). The mechanical properties were measured using a standard strain test. It was found that with the incorporation of HEPFA, PDMS, and sol–gel solution into the polyurethane basecoat (B), the tensile modulus and tensile strength of the coatings were significantly increased, but the elongation at break of the coatings were decreased. This was due to the denser

Table 6 Mechanical properties of UV-cured hybrid coatings

Samples	Tensile modulus (*E*), (MPa)	Tensile strength (MPa)	Elongation at break (Ɛ), (%)
B	169	94	18.1
B/S10	215.4	125.3	16.1
B/S20	222.1	141.3	12.1
B/S30	240.2	153	12
H20	238.3	127	16
H20/S10	253	131.2	12
H20/S20	259	135	10.2
H20/S30	274	159.1	11.2
H40	262.1	147	14
H40/S10	281.1	151.1	11.2
H40/S20	315.1	161.1	15
H40/S30	335	172.1	9.2
P10:H20	287.2	167.1	15
P10:H20/S10	315.1	169.2	15.2
P10:H20/S20	327	191.2	8.3
P10:H20/S30	338.1	209.3	10
P20:H40	310.1	185.3	12.1
P20:H40/S10	321.1	200.3	14.1
P20:H40/S20	329.2	235.1	9
P20:H40/S30	343	255.3	6.2

crosslinking of the nano-hybrid coatings as well as the improvement in the stiffness of the PUAs with bulky aromatic HEPFA groups. The fluorinated aromatic rings, which also contain rigid 6F groups, restrict the mobility of the chain and caused a decrease in flexibility.

Conclusion

In this study, five different UV-curable fluorine—and siloxane-containing polyurethane acrylate coating materials were successfully synthesized by using HEPFA and PDMS as building blocks in the PUAs. The nano-hybrid formulations were prepared by adding 10–30 wt% sol–gel solution in the PUA formulations. The introduction of HEPFA into the molecular chain of the PUA formulations (H20/S10-S30, H40/S10-S30 P10:H20/S10-S30, P20:H40/S10-S30) significantly improved the coating materials in terms of hardness, contact angle values and thermal properties. We also incorporated siloxane bonds into the molecular structure of PUAs (P10:H20/S10-S30, P20:H40/S10-S30). PDMS showed a remarkable effect on the gloss and hardness of the coatings. These results can be attributed to the addition of flexible siloxane bonds and rigid –CF3 groups which is also attached to the aromatic rings

into the molecular structure of PUAs. Moreover, the best results were obtained with higher sol–gel content for the PUA nano-hybrid formulations, which formed stable Si–O–Si networks by TEOS and VTMS. This can also be attributed to the similarity between the PDMS and the sol–gel solution, which promotes compatibility between the PUA matrix and the sol–gel solution and leads to uniform distribution in the nano-hybrid formulations, which is improving its morphological properties. In this study, P20:H40 and its nano-hybrid P:20/H:40/S30 showed the best coating performance in the group of synthesized PUA coatings in terms of mechanical, physical, morphological and thermal properties. Since PDMS, HEPFA and sol–gel content together had good synergistic effects, the coating material exhibited good adhesion, hardness and gloss, and also showed improvements in physical properties. Based on these results, fluorine—and silicone-containing polyurethane acrylates could be candidates for coating materials in practical applications.

Acknowledgements This work was supported by Marmara University Science Fund. (BAP No: FEN-C-YKP-080415-012).

References

1. Engels HW, Pirkl HG, Albers R, Albach RW, Krause J, Hoffmann A et al (2013) Polyurethanes: versatile materials and sustainable problem solvers for today's challenges. Angew Chem Int Ed 52:9422–9441. https://doi.org/10.1002/anie.201302766
2. Golling FE, Pires R, Hecking A, Weikard J, Richter F, Danielmeier K, Dijkstra D (2018) Polyurethanes for coatings and adhesives—chemistry and applications. Polym Int 68:848–855. https://doi.org/10.1002/pi.5665
3. Eling B, Tomović Ž, Schädler V (2020) Current and future trends in polyurethanes: an industrial perspective. Macromol Chem Phys 221:2000114. https://doi.org/10.1002/macp.202000114
4. Qian Y, Lindsay CI, Macosko C, Stein A (2011) Synthesis and properties of vermiculite-reinforced polyurethane nanocomposites. ACS Appl Mater Interfaces 3:3709–3717. https://doi.org/10.1021/am2008954
5. Chattopadhyay DK, Raju KVSN (2007) Structural engineering of polyurethane coatings for high performance applications. Prog Polym Sci 32:352–418. https://doi.org/10.1016/j.progpolymsci.2006.05.003
6. Chattopadhyay DK, Webster DC (2009) Thermal stability and flame retardancy of polyurethanes. Prog Polym Sci 34:1068. https://doi.org/10.1016/j.progpolymsci.2009.06.002
7. Bai C, Zhang X, Dai J, Wang J (2008) Synthesis of UV crosslinkable waterborne siloxane–polyurethane dispersion PDMS-PEDA-PU and the properties of the films. J Coat Technol Res 5:251–257. https://doi.org/10.1007/s11998-007-9062-8
8. Amrollahi M, Sadeghi GMM (2016) Assessment of adhesion and surface properties of polyurethane coatings based on non-polar and hydrophobic soft segment. Prog Org Coat 93:23–33. https://doi.org/10.1016/j.porgcoat.2015.12.001
9. Fu J, Wang L, Yu H, Haroon M, Haq F, Shi W, Wang L (2019) Research progress of UV-curable polyurethane acrylate-based hardening coatings. Prog Org Coat 131:82–99. https://doi.org/10.1016/j.porgcoat.2019.01.061
10. Bongiovanni R, Di MA, Pollicino A, Priola A, Tonelli C (2008) New perfluoropolyether urethane methacrylates as surface modifiers: Effect of molecular weight and end group structure. React Funct Polym 68:189–200. https://doi.org/10.1016/j.reactfunctpolym.2007.09.009
11. Yagci Y, Jockusch S, Turro NJ (2010) Photoinitiated polymerization: advances, challenges, and opportunities. Macromolecules 43:6245–6260. https://doi.org/10.1021/ma1007545
12. Fu J, Wang L, Yu H, Haroon M, Haq F, Shi W et al (2019) Research progress of UV-curable polyurethane acrylate-based hardening coatings. Prog Org Coat 131:82–99. https://doi.org/10.1016/j.porgcoat.2019.01.061

13. Tasic S, Bozic B, Dunjic B (2004) Synthesis of new hyperbranched urethane-acrylates and their evaluation in UV-curable coatings. Prog Org Coat 51:320–327. https://doi.org/10.1016/j.porgcoat.2004.07.021
14. Um MS, Ham DS, Cho SK, Lee SJ, Kim KJ, Lee JH et al (2016) Surface mechanical properties of poly(urethane acrylate)/silica hybrid interpenetrating polymer network (IPN) coatings. Prog Org Coat 97:166–174. https://doi.org/10.1016/j.porgcoat.2016.04.007
15. Jiao Z, Wang X, Yang Q, Wang C (2017) Modification and characterization of urethane acrylate oligomers used for UV-curable coatings. Polym Bull 74:2497–2511. https://doi.org/10.1007/s00289-016-1847-4
16. Kaewpirom S, Kunwong D (2012) Curing behavior and cured film performance of easy-to-clean UV-curable coatings based on hybrid urethane acrylate oligomers. J Polym Res 19:1–12. https://doi.org/10.1007/s10965-012-9995-1
17. Tielemans M, Roose P, Ngo C, Lazzaroni R, Leclère P (2012) Multiphase coatings from complex radiation curable polyurethane dispersions. Prog Org Coat 75:560–568. https://doi.org/10.1016/j.porgcoat.2012.05.010
18. Jena KK, Narayan R, Raju KVSN (2013) New high performance waterborne organic–inorganic hybrid materials from UV curing. Prog Org Coat 76:1418–1424. https://doi.org/10.1016/j.porgcoat.2013.04.014
19. Kayaman-Apohan N, Demirci R, Cakir M, Gungor A (2005) UV-curable interpenetrating polymer networks based on acrylate/vinylether functionalized urethane oligomers. Radiat Phys Chem 73:254–262. https://doi.org/10.1016/j.radphyschem.2004.09.026
20. Mammeri F, Bourhis EL, Rozes L, Sanchez C (2005) Mechanical properties of hybrid organic–inorganic materials. J Mater Chem 15:3787. https://doi.org/10.1039/b507309j
21. Jang ES, Khan SB, Seo J, Akhtar K, Choi J, In-Kim K, Han H (2011) Synthesis and characterization of novel UV-Curable PU-Si hybrids: Influence of silica on thermal, mechanical, and water sorption properties of polyurethane acrylates. Macromol Res 19:1006–1013. https://doi.org/10.1007/s13233-011-1002-x
22. Karataş S, Kayaman-Apohan N, Turunç O, Güngör A (2011) Synthesis and characterization of UV-curable phosphorus containing hybrid materials prepared by sol-gel technique. Polym Adv Technol 22:567–576. https://doi.org/10.1002/pat.1546
23. Cho J-D, Ju H-T, Hong J-W (2004) Photocuring kinetics of UV-initiated free-radical photopolymerizations with and without silica nanoparticles. J Polym Sci Part A 43:658–670. https://doi.org/10.1002/pola.20529
24. Luo Z, Hong RY, Xie HD, Feng WG (2012) One-step synthesis of functional silica nanoparticles for reinforcement of polyurethane coatings. Powder Technol 218:23–30. https://doi.org/10.1016/j.powtec.2011.11.023
25. Najafi F, Bakhshandeh E, Hadavand BS, Saeb MR (2014) Toward UV-curable urethane acrylate/silica hybrid coatings: introducing urethane methacrylate trimethoxysilane (UAMS) as organic–inorganic coupling agent. Prog Org Coat 77:1957–1965. https://doi.org/10.1016/j.porgcoat.2014.07.002
26. Zheng G, Lu M, Rui X (2017) The effect of polyether functional polydimethylsiloxane on surface and thermal properties of waterborne polyurethane. Appl Surf Sci 399:272–281. https://doi.org/10.1016/j.apsusc.2016.12.047
27. Zhang S, Chen Z, Guo M, Bai H, Liu X (2015) Synthesis and characterization of waterborne UV-curable polyurethane modified with side-chain triethoxysilane and colloidal silica. Colloids Surf A 468:1–9. https://doi.org/10.1016/j.colsurfa.2014.12.004
28. Pergal M, Nestorov J, Tovilovic-Kovacevic G et al (2014) Surface characterization, hemo—and cytocompatibility of segmented poly(dimethylsiloxane)-based polyurethanes. Chem Ind 68:731–741. https://doi.org/10.2298/hemind141103082p
29. Zhang S, Chen Z, Guo Z, Zhao J, Liu X (2014) Waterborne UV-curable polycarbonate polyurethane nanocomposites based on polydimethylsiloxane and colloidal silica with enhanced mechanical and surface properties. RSC Adv 4:30938. https://doi.org/10.1039/c4ra03842h
30. Pergal MV, Dzunuzovic JV, Poreba R, Micic D, Stefanov P, Pezo L, Spirkov M (2013) Surface and thermomechanical characterization of polyurethane networks based on poly(dimethylsiloxane) and hyperbranched polyester. Express Polym Lett 7:806–820. https://doi.org/10.3144/expresspolymlett.2013.78
31. Król B, Król P, Byczyński Ł, Szałański P (2017) Methods of increasing hydrophobicity of polyurethane materials: important applications of coatings with low surface free energy. Colloid Polym Sci 295:2309–2321. https://doi.org/10.1007/s00396-017-4202-x

32. Li N, Zeng FL, Wang Y, Qu D, Zhang C, Li J, Huo J, Bai Y (2018) Synthesis and characterization of fluorinated polyurethane containing carborane in the main chain: thermal, mechanical and chemical resistance properties. Chin J Polym Sci 36:85–97. https://doi.org/10.1007/s10118-018-2014-1
33. Ping T, Zhou Y, He Y, Tang Y, Yang J, Akram MY, Nie J (2016) Preparation and characterization of yellowing resistance and low volume shrinkage of fluorinated polysiloxane urethane acrylate. Prog Org Coat 97:74–81. https://doi.org/10.1016/j.porgcoat.2016.03.023
34. Yan Z, Liu W, Gao N, Ma Z, Han M (2013) Synthesis and characterization of a novel difunctional fluorinated acrylic oligomer used for UV-cured coatings. J Fluor Chem 147:49–55. https://doi.org/10.1016/j.jfluchem.2013.01.014
35. Qi Y, Li K, Li K, Li K, Hu B, Wang X (2017) The influence of tiny amount fluorine-containing acrylate on kinetics, morphology and properties free-radical/cationic hybrid UV-cured coatings. Prog Org Coat 112:44–50. https://doi.org/10.1016/j.porgcoat.2017.06.026
36. Wang L-F (2007) Experimental and theoretical characterization of the morphologies in fluorinated polyurethanes. Polymer 48:894–900. https://doi.org/10.1016/j.polymer.2006.11.063
37. Yu Y, Liao B, Jiang S, Li G, Sun F (2015) Synthesis and characterization of photosensitive-fluorosilicone–urethane acrylate prepolymers. Des Monomers Polym 18:199–209. https://doi.org/10.1080/15685551.2014.999458
38. Ge Z, Zhang X, Dai J, Li W, Luo Y (2009) Synthesis, characterization and properties of a novel fluorinated polyurethane. Eur Polym J 45:530–536. https://doi.org/10.1016/j.eurpolymj.2008.11.008
39. Çakır Çanak T, Serhatlı İ (2013) Synthesis of fluorinated urethane acrylate based UV-curable coatings. Prog Org Coat 76:388–399. https://doi.org/10.1016/j.porgcoat.2012.10.024
40. Smirnova O, Glazkov A, Yarosh A, Sakharov A (2016) Fluorinated polyurethanes, synthesis and properties. Molecules 21:904. https://doi.org/10.3390/molecules21070904
41. Wang X, Xu J, Li L, Liu Y, Li Q (2016) Influences of fluorine on microphase separation in fluorinated polyurethanes. Polymer 98:311–319. https://doi.org/10.1016/j.polymer.2016.06.039
42. Zhang L, Zeng Z, Yang J, Chen Y (2004) Characterization and properties of UV-curable polyurethane-acrylate/silica hybrid materials prepared by the sol-gel process. Polym Int 53:1431–1435. https://doi.org/10.1002/pi.1536
43. Liu F, Liu A, Tao W, Yang Y (2020) Preparation of UV curable organic/inorganic hybrid coatings-a review. Prog Org Coat 145:105685. https://doi.org/10.1016/j.porgcoat.2020.105685
44. Qiu F, Xu H, Wang Y, Xu J, Yang D (2012) Preparation, characterization and properties of UV-curable waterborne polyurethane acrylate/SiO2 coating. J Coat Technol Res 9:503–514. https://doi.org/10.1007/s11998-012-9397-7
45. Topçu G, Baştürk E, Karataş S (2018) Effects of perfluoro modified sol-gel additive on UV-curable phosphorus containing urethane acrylate coatings. J Vinyl Add Tech 24:E133–E145. https://doi.org/10.1002/vnl.21616
46. Zhu C, Yang H, Liang H, Wang Z, Dong J, Xiong L et al (2018) A novel synthetic UV-curable fluorinated siloxane resin for low surface energy coating. Polymers 10:979. https://doi.org/10.3390/polym10090979
47. Zhou J, Zhu C, Liang H, Wang Z, Wang H (2020) Preparation of UV-curable low surface energy polyurethane acrylate/fluorinated siloxane resin hybrid coating with enhanced surface and abrasion resistance properties. Materials 13:1388. https://doi.org/10.3390/ma13061388

Authors and Affiliations

Mert Çınar[1] · **Sevim Karataş**[1]

[1] Department of Chemistry, Faculty of Arts and Science, Marmara University, 34722 Göztepe, Kadıköy, Istanbul, Turkey